OXIDANT TRANSPORT THROUGH EUROPA'S ICE SHELL BY BRINE DRAINAGE FROM CHAOTIC TERRAINS. M. A. Hesse[1], J. S. Jordan[2], S. D. Vance[3], and C. McCarthy[4]. [1]Department of Geological Science, The University of Texas at Austin, Austin TX 78712, USA (e-mail address: mhesse@jsg.utexas.edu),[2]Department of Earth, Environmental and Planetary Sciences, Rice University, Houston TX 77005 , [3]Jet Propulsion Laboratory, California Institute of Technology, Pasadena, CA 91109, USA, [4]Lamont-Doherty Earth Observatory, Columbia University, Palisades NY 10964.

Introduction: The habitability of Europa's interior ocean depends, among other conditions, on the availability of redox gradients [1,2]. High oxidant fluxes are likely only if oxidants produced at the surface [3] can be transported through the ice shell into the ocean. However, the transport mechanisms and the resulting fluxes of oxidants are currently not clear. Convective overturn of the ice shell is an obvious mechanism for oxidant transport [4, 5]. However, an intensive search for subduction features in the surface geology, has yielded the identification of only one relatively small subducted area [6]. This suggests that convective overturn is currently not an effective mechanism for oxidant transport through the ice shell.

Oxidant transport by brine percolation: Another possibility is the transport of oxidants by the downward migration of dense brines formed by partial melting of the ice near the surface [7, 8, 9]. Here, we investigate the drainage of near surface bines, which are thought to be generated during the formation of chaotic terrains [10]. This mechanism could deliver significant amounts of oxidants to the ocean, because chaotic terrains cover on quarter of Europa's surface [11] and it is possible that large quantities of brine are created during their formation [12].

Brine percolation through the ice shell Brine percolation requires that the ice below the conductive lid is permeable. The geotherm in Figure 1a shows that temperatures in the convective portion of the ice shell exceed the eutectic temperature with sodium chloride salts. The estimated salt contents of Europa's ice, between 0.01 and 0.1 wt% suggest melt fractions/brine filled porosities of approximately 10^{-3} to 10^{-2} in the convective ice shell. However, it is not clear if this porosity is connected and allows flow. While rapidly formed sea ice generally has a percolation threshold at 0.05 (Figure 1b), typical brines wet the ice grain boundaries and are expected to form connected melt networks at textural equilibrium [16]. Here we assume that the small melt fraction in the convective portion of the ice shell percolates and that the permeability is given by power law relations from textural equilibrium [15]. In this case, any near surface brine drains into the ocean unless it refreezes in place.

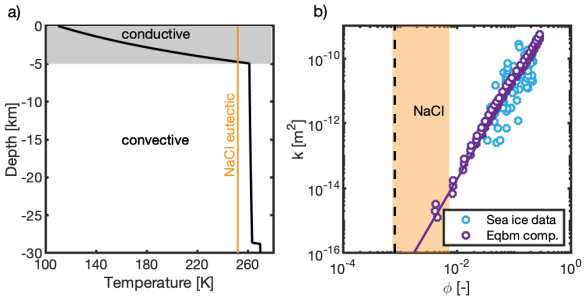

Figure 1: a) Geotherms in Europa's icy lithosphere for a cold ocean [13] with the eutectic temperature for the H_2O-NaCl system. b) Permeability-porosity power law for brine in ice [14, 15]. Shaded area shows likely melt fractions due to salt, dashed line the assumed background melt fraction in the ice.

Model problem: Here we study a simplified model problem to determine if near surface brines can drain before they refreeze. We study the following simplified scenario: A convective ice shell with 3 wt% NaCl is overlain by a conductive lid with 0.01 wt% NaCl. We assume that some unspecified chaos-forming process has brought convective temperatures to the surface, so that the entire ice shell is initially at the mean temperature of the convective portion, ~262 K. This leads to a melt fraction of 0.23 in the near surface underlain by ice with a porosity of $8 \cdot 10^{-4}$. We also assume the entire near-surface high-porosity region is saturated by oxidant. This is either due to the presence of oxidants throughout this depth before melting, or due to some unspecified vigorous mixing process during chaos formation.

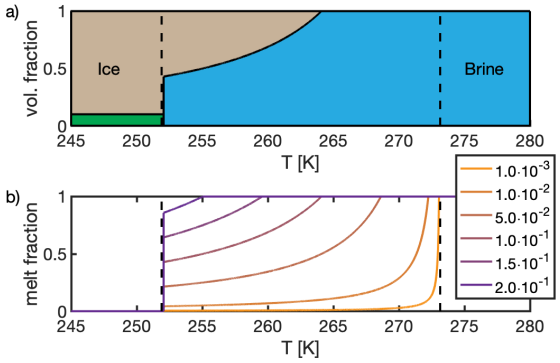

Figure 2: a) Volume fractions of ice (teal), hydrohalite (green) and brine (blue) for 10 wt% NaCl as a function of temperature. b) Melt fraction as a function of temperature for increasing salt contents in eutectic melting.

Model for brine drainage and refreezing: To model the refreezing during brine drainage we have extended the Enthalpy Method [8, 17] to the binary H_2O-NaCl eutectic. This allows us to model the strong coupling between salt content and the melt fraction (Figure 2). This model for the phase behavior is coupled to a mechanical model for brine drainage through ductile ice [18]. The phase velocities from the mechanical model are then used to update the bulk composition and enthalpy of the system, which in turn determine temperature and volume fractions of ice, salt and brine.

Results: Here we present one-dimensional results for the coupled drainage and refreezing dynamics for the model problem outlined above. Results for an ice shell with shear viscosity of $2 \cdot 10^{15}$ Pa s and permeability of 10^{-17} m^2 are shown in Figure 3. Refreezing is too slow to arrest the drainage of the brine and prevent the oxidant delivery to the internal ocean. The delivery timescale for oxidants is 20 ka after the formation of the near surface brine.

Formation of subterranean lakes near the surface. The main mechanism that prevents the refreezing, is the rapid segregation of the brine to the bottom of the near-surface high-porosity region at 3 km depth (Figure 3b). The formation of this "perched aquifer" [12] is completed in less than 3 ka, because the high porosity weakens the resistance to dilation. Freezing is only fast enough to trap brine in the top kilometer of the ice shell, through precipitation of salt at the eutectic temperature (Figure 3c). Hence the bulk of the near-surface melt is effectively removed from the immediate reach of the freezing front. The porosities at the base of the near surface melt layer reach 0.7 and suggest the formation of subterranean lake where the remaining ice likely floats to the top.

Formation of porosity waves in the convective ice shell. The high pore pressures at the base of the subterranean lake slowly dilates the underlying convective ice shell, allowing the brine to drain. After approximately 6 ka, a porosity wave forms and propagates downward with constant velocity (Figure 3b). Porosities in this wave reach 0.24 and the wave propagates an order of magnitude faster than the drainage velocity in the low permeability background. such porosity waves are common features of brine percolation in ductile ice [8, 14].

Downward oxidant transport. This porosity wave transports the bulk of the oxidants initially contained in the subterranean lake. Figure 3d shows the oxidant concentration profiles in the brine, normalized to an appropriate near-surface abundance. An oxidant front propagates with the speed of the porosity wave and reaches the base of the ice shell after approximately 20 ka.

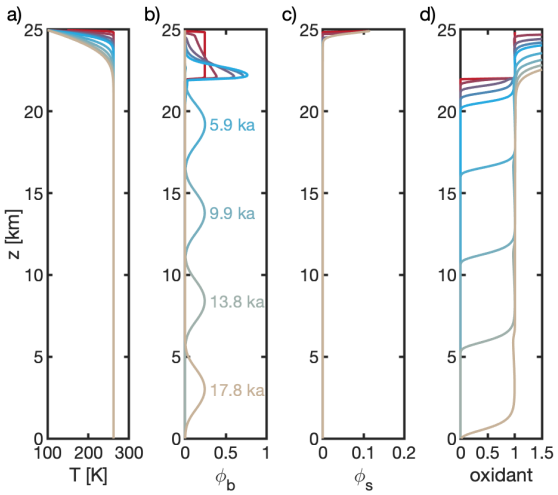

Figure 3: Simulation of brine drainage and refreezing. Results are shown at intervals of 400 yrs for 2800 yrs (red to blue) followed by intervals of 4000 yrs until 20 ka (blue to tan): a) Temperature profiles. b) Melt fraction/porosity. c) Salt (Hydrohalite) volume fraction. d) Normalized oxidant concentration.

The bulk of the oxidants are delivered with the arrival of the porosity waves. The conclusion that refreezing does not prevent the downward oxidant transport appears robust for a reasonable set of ice shell parameters, but is predicated on the percolation of small melt fractions. Thus the overall rate of oxidant delivery is likely determined by near-surface melting (e.g., through chaos formation) rather than the transport through the ice shell.

References: [1] Chyba C. F. and Phillips C. B. (2001) *PNAS*, 98(3), 801-804. [2] Vance S. D. et al. (2016) *GRL*, 43(10), 4871-4879. [3] Carlson et al. (1999) *Science*, 283, 2062-2064. [4] Pappalardo R. T. et al. (1998) *Nature*, 391, 365-368. [5] McKinnon W. B. (1999) *Geophys. Res. Lett.* 26(7), 951-954. [6] Kattenhorn S. A. and Prockter L. M. (2014) *Nat Geosci*, 7, 762-767. [7] Barr A. et al. (2002) *LPSC 33*, Abstract 1545. [8] Hesse et al. (2019) *LPSC 50*, Abstract# 1489. [9] Hesse et al. (2019) Ocean Worlds 4, Abstract# 6019. [10] Collins et al. (2000) *JGR*, 105, 1709-1716. [11] Senske, D.A. et al. (2018) LPSC 49, Abstract# 1340. [12] Schmidt B. E., et al. (2011) *Nature*, 479(7374), 502-505. [13] Vance S. D. et al. (2018), *JGR-Planets*, 123(1), 180-205. [14] Kalousova K. et al. (2014) *JGR-Solid Earth*, 119(3), 532-549. [15] Ghanbarzadeh et al. (2017), PNAS, 114(51), 13406-13411. [16] De La Chapelle et al. (1999), *Geophys. Res Lett.*, 26(2), 251-254. [17] Hesse M. A. and Jordan J. S. (2016), *Geochem. Geophys. Geosyst*. 16. [18] Jordan et al. (2018) *EPSL*, 485, 65-78.